Porcine Bone Marrow Stromal Cell Differentiation on Heparin-Adsorbed Poly (e-Caprolactone)-Tricalcium Phosphate-Collagen Scaffolds

Zhi Zhen Chum [1,] *Maria A. Woodruff* [2,] *Simon M Cool* [3,4] *and*

**Dietmar W. Hutmacher* [2]

[1]Division of Bioengineering, Faculty of Engineering, National University of Singapore, Singapore 119260
[2]Institute of Health and Biomedical Innovation, Queensland University of Technology, 60 Musk Avenue, Kelvin Grove, Brisbane, 4059. *Corresponding Author: Phone: 07 3138 6077| Fax: 07 3138 6030 | International: +61 7 3138 6077
Dietmar.Hutmacher@qut.edu.au.
[3]Department of Orthopaedic Surgery, Yong Loo Lin School of Medicine, National University of Singapore, 119074.
[5]*Stem Cells and Tissue Repair Group, Institute of Medical Biology, A*STAR, Immunos, Singapore 138648;*

Scaffold, PCL-Collagen, Cell Differentiation, Heparin

INTRODUCTION

Mesenchymal progenitor cells are the principal cells contributing to bone formation by virtue of their ability to differentiate into osteoblasts [1]. The multi-step transformation of progenitor cells into bone-forming cells involves the complex interaction of a variety of growth factors and cell signalling molecules. The majority of extracellular signals that guide cells through these types of phenotypic progressions bind to the particular class of carbohydrates that is prominent in the extracellular matrix of growing and repairing tissues. Heparan sulfate (HS) and heparin are members of the glycosaminoglycan (GAG) family of polysaccharides, and the importance of HS to bone is best explained by its ability to bind and bioactivate most of the growth and adhesive factors involved in regulating bone cell metabolism and osteoblast lineage progression [2, 3]. Although constituted by the same disaccharide building blocks (though in different proportions), compared to heparin, HS is less sulfated, more heterogeneous and present on the surface of most cell types and in the extracellular matrix (ECM), while the hyper-sulfated anti-coagulant, heparin, is usually sequestered in mast cells [4]. The ECM-resident HS acts to concentrate growth factors close to cell surfaces, protecting them from extracellular proteases, and facilitating binding to their specific receptors in an active form [3]. Heparin, both commercially and readily available, is often used to approximate HS action (albeit with reduced specificity), and has been shown clinically to interfere with the ligand-binding activities of HS by competitively inhibiting the susceptible factors needed by osteoblasts [5, 6], leading to an osteoporotic-like reduction in bone formation [7-9]. Various molecular mechanisms have been proposed for these observations, including the enhancement of interleukin-11 signalling through an up-regulation of the MAPK pathway [10]. However, a recent two-dimensional (2D) cell culture study has shown that although high concentrations of heparin can lead to a reduction in cell numbers with inhibited matrix deposition and mineralization, almost certainly by non-specific competition with endogenous HS, low concentrations of heparin (5 - 500 ng/ml) actually promote ECM deposition and mineralization in osteoblast-like Saos-2 cells [11]. Thus heparin may exert biphasic effects, and it appears that low doses

might actually be beneficial for bone formation by potentiating local growth factors. However, the aforementioned study has two disadvantages; namely it was performed with an osteosarcoma cell line, and ~~on it was~~ on a 2D surface. Biomedicine has become increasingly aware of the limitations of conventional 2D cell culture. This has greatly intensified the pace by which 3D cell culture systems have been developed; it is an environment that might be considered to occupy the space between a Petri dish and a mouse. Although traditional culture dishes have had an enormous impact on modern biology, the Petri dish and its ancillaries including multiwell plates and glass cover slips, are less than ideal to study cells and tissues. The Petri dish surface is rigid and inert without coating, as opposed to the *in vivo* "soft" environment where cells interact intimately with the ECM and with each other in three-dimensions. Intracellular transport phenomena between 2D and 3D are drastically different. In 2D culture systems, cytokines, chemokines, and growth factors quickly diffuse in the media across the culture dish, whereas the *in vivo* environment benefits from chemical and biological gradient diffusion systems, which play a vital role in signal transduction, cell–cell communications and development.

The use of mesenchymal progenitor cells (MPCs) for preclinical *in vivo* studies, wherein they are implanted into critical-sized bone defects, is the subject of much interest [12], particularly when they employ large-animal, load-bearing immunocompetent models [13]. The characterisation of MPCs within this context is of great importance, especially considering the potential availability of large numbers of immune-privileged, harvestable cells and the similarity in the mechanical features of the bone biology in comparison to humans. Although studies have been published on the characterisation of porcine bone marrow mesenchymal stem/stromal cells (MPCs) [14], the specific biochemical cues influencing their osteogenic differentiation in 3D culture systems and on specific substrates have been explored to a much lesser extent [15].

The aims of the present study were two-fold. First, we sought to explore the ability of porcine MPCs to differentiate into either the osteogenic or adipogenic lineages within a 2D tissue culture plate

system. Secondly, we sought to determine the effect of heparin on porcine MPCs seeded onto poly (e-caprolactone)-tricalcium phosphate-collagen type I **(**PCL-TCP-Col) 3D scaffolds.

The study thus aimed to evaluate the potential use of 3D PCL-TCP-Col scaffolds for future *in-vivo* applications. It also aimed to investigate whether the inclusion of heparin as a substrate would improve this system, particularly pertaining to bone tissue engineering by investigating it's effect on the bone-forming potential of porcine MPCs.

MATERIALS AND METHODS

Progenitor cell extraction, culture conditions and cell seeding

Bone marrow precursor cells (MPCs) were isolated from 10 - 15 ml of marrow aspirated from 16-week old Duroc/ Yorkshire Cross pigs using strict aseptic techniques. Progenitor cells were isolated by plating the freshly aspirated bone marrow onto polystyrene T-150 culture flasks (approx 5ml of aspirate per flask). (Nalgen-Nunc, Denmark) in 30 ml control medium consisting of Dulbecco`s Modified Eagle Medium (DMEM:low glucose), 10% fetal bovine serum and 1% penicillin-streptomycin and incubated at 37^{o}C in a humidified atmosphere containing 5% CO_2 (Binder, Tuttlingen Germany). Non-adherent cells were removed at day 4 and the culture media changed every 3 - 4 days and this was continued until the cells attained 70% confluence. BMSCMPCs were then utilised either in 2D studies (for osteogenic and adipogenic assays), or seeded onto 3D PCL-TCP-Col scaffolds (with and without the addition of heparin) and observed for their bone tissue engineering capabilities.

Two dimensional studies : adipogenic and osteogenic induction:

For adipogenic induction, cells in their 3rd passage were plated in control media at a density of 5000 cells/cm^2 and on the 2nd day of culture treated with adipo-induction media [(control medium containing 1 mM dexamethasone (1 mM stock in 100% ethanol), 0.2 mM indomethacin (100 mM stock in 100% ethanol), 0.01 mg/ml insulin, 0.5 mM 3-isobutyl-1-methylxanthine (500 mM stock in DMSO)]. The adipo-induction media was replaced every 3 - 4 days and was continued for 6 weeks. The adipogenic differentiation was visually monitored by phase-contrast microscopy and the formation of lipid-filled vacuoles confirmed by Oil-Red-O staining. For staining, cells were fixed with 4% (w/v) formaldehyde/1% (w/v) calcium, washed with 70% ethanol and incubated with 2% (w/v) Oil-Red-O (Sigma Aldrich; St Louis, USA) for 5 min at room temperature. Excess stain was then removed by further washing with 70 % ethanol then diH_20). Counterstaining was performed with

Meyer's hematoxylin (H&E; Sigma Aldrich; St Louis, USA). For quantitation, 10 randomly chosen, non-overlapping, low power micrographs of each sample were taken; the positive cells were counted and compared with the total cell number.

For osteogenic induction, cells in their 3rd passage were plated in control medium at a density of 3000 cells/cm^2 and on the 2nd day of culture treated with osteo-induction media [(control medium containing 0.1 mM ascorbic acid 2-phosphate, 10 mM β-glycerophosphate, 100 nM dexamethasone (1 mM stock in 100% ethanol)]. The medium was then replaced every 3-4 days and was continued for 4 weeks. Osteogenic differentiation was then determined using Alizarin Red staining to assess calcium deposits. Briefly, samples were rinsed twice in PBS, fixed with 10% formalin for 10 min at room temperature, and rinsed with diH_20. Alizarin Red (pH 5.5, adjusted by ammonium hydroxide) (Sigma Aldrich; St Louis, USA) solution was added for 30 min ~~sec~~, and then the wells drain and washed with diH_20 until clean.

The morphology of the cells under the different conditions was also observed by light microscopy (Leica DM IRB, Germany) following H&E staining.

Three dimensional studies: Collagen lyophilisation and heparin adsorption on PCL-TCP scaffolds

Scaffolds made from medical grade 80% PCL-20% TCP (Osteopore International, Singapore) were fabricated by fused deposition modeling [16] and were punched from a stock sheet yielding scaffolds 1 mm thick and 5 mm in diameter with a 0 - 90^o lay down pattern and porosity of 70%. Scaffolds were next treated with 5 M NaOH for 3 h at 37^{o}C followed by washing with PBS and drying overnight in order to make the surface more hydrophilic and to facilitate better cell attachment [17]. Rat tail Collagen type I (5 mg/ml in 0.5 M acetic acid, Sigma) was neutralised by 71.2 mg/ml sodium bicarbonate (volume ratio of collagen:sodium bicarbonate was 100:9). The mixture (70 µl) was added onto the NaOH-treated scaffolds that were then placed into 96-well plates. The scaffolds were left at room temperature for 30 min and then frozen at -80^{o}C for 3 days, followed by lyophilisation using a freeze dryer for 24 h. Scaffolds were then stored in a dry cabinet.

In order to investigate the effects of heparin on osteogenic differentiation in a 3D environment, the scaffolds were divided into two groups. The control group was lyophilised with collagen alone, and the second group was lyophilised with collagen and then coated with heparin. For heparin adsorption, PCL-TCP-Col scaffolds were placed in the wells of a 96-well plate and sterilized under UV (1h). Heparin (10 µl of 0.1 mg/ml; sodium salt from porcine intestinal mucosa (Sigma) diluted in sterile PBS) was then added onto the scaffold and left at 4^{o}C overnight. Cells were then seeded onto each scaffold suspended within specially cut micropipette tips so as to prevent contact with the bottom of the culture wells, and placed into 24-well culture plates (Fig. 1). For osteogenic induction, cells were seeded at a density of 3000 cells/cm^2 (10 µl cell suspension containing approximately 0.1 X 10^6 cells), and incubated at 37°C for 1.5 h to facilitate cell attachment, followed by treatment with osteo-induction medium.

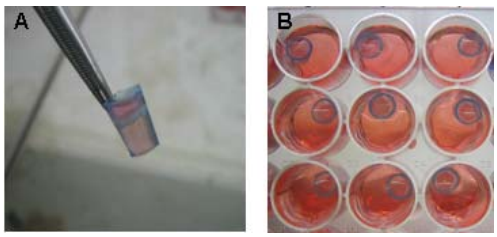

Figure 1. Scaffold suspended in media within the modified pipette tip (A). Placed inside the 24-well culture plate (B).

Heparin-alexa conjugate

To enable visualisation of the distribution of heparin within the scaffolds, a heparin-AlexaFluor hydrazide conjugate was prepared based on the method modified from Osmond et al. [18] Briefly, 50 µl of the EDC solution (10% w/v solution of EDC up in an 0.1 M MES buffer, pH 4.5) (Sigma) was added to 300 µl of heparin solution (3 mg of heparin in 300 µl of MES buffer at pH 4.5) and vortexed. AlexaFlour488 (0.5 mg) (Molecular Probes) was added to the heparin/EDC mixture and incubated overnight at room temperature. The solution was passed through an Amersham PD10 column following the manufacturer's instructions using water as the elution buffer. The Heparin-Alexa

solution was concentrated by freeze-drying and stored at 4^{o}C protected from light. The conjugated heparin was added to each scaffold in the manner described above.

Confocal laser scanning microscopy

Confocal laser scanning microscopy was used to determine the extent of adsorption of heparin onto the scaffolds lyophilised with collagen, and also to assess the viability of cells within the cell-scaffold constructs. For assessment of cell viability, the cell-scaffold constructs were rinsed twice with sterile PBS, incubated with 2 µg/ml fluorescein diacetate (FDA) (molecular probes) in PBS for 15 min at 37 °C, then rinsed again twice with PBS. Propidium iodide (PI) (20 µg/ml) (molecular probes) in PBS was added for 2 min at room temperature followed by washing with PBS. All steps were performed in the dark and samples were then viewed under a Zeiss (LSM510 META) confocal laser microscope.

Cell metabolism: Alamar blue assay

Cellular metabolism was assessed by the alamar blue assay, wherein dye reduction was considered proportional to the metabolic activity of the cells. Assay media (2 ml of 10% (v/v) alamar blue (Probes, OR, USA)) was used. After 3 h incubation, 100 µl of assay media was transferred to a 96-well plate and absorbance at 570 nm and 600 nm was determined on a microplate reader (Magellan) and the percentage reduction of the dye calculated.

Cell proliferation: PicoGreen assay

PicoGreen dsDNA quantitation kits (Molecular Probes Inc., USA) were used to measure cell proliferation by quantitating the amount of double-stranded DNA (dsDNA) in solution. Samples were washed twice with PBS and stored at -80^{o}C until use. Samples were later thawed and the enzymatic cocktail (0.1% w/v collagenase + 0.1% v/v trypsin) was added into the culture wells and incubated for 1 h at 37^{o}C; the samples were mixed by a micropipette every 15 min to ensure complete cell detachment and lysis. Each sample was aliquotted into 3 x 1 mL microcentrifuge tubes and a 1:20

dilution in TE buffer was performed. Samples from each tube were then aliquoted into a 96-well plate in triplicates (3 X 100 µl) and incubated with 100 µl of picoGreen working solution, 1:200, for 5 min at room temperature, protected from light. Fluorescence of the whole sample mixture was measured at excitation and emission wavelengths of 480 and 520 nm, respectively on a microplate reader (Fluostar).

For 3D cell-scaffold constructs, the specimens were washed twice with PBS and placed into cryogenic vials, which were immersed into liquid nitrogen for 30 s. The samples were then stored at -80^{o}C until later thawed and cut into small pieces. Autoclaved deionised H_2O (200 µl) was added into each vial and the cells lysed using 3 cycles of snap-freezing in liquid nitrogen, with agitation between each step to ensure all cells were lysed, followed by thawing to room temperature. Each sample was aliquotted into 3 x 1mL microcentrifuge tubes in a 1:10 dilution in TE buffer. Samples from each tube were then aliquotted into a 96-well plate in triplicates (3 X 100 µl) and incubated with 100 µl of picoGreen working solution, 1:200, for 5 min at room temperature, protected from light and fluorescence determined as described above.

Alkaline phosphatase activity

Triplicates of the supernatant from both the heparin-coated and non-coated groups were collected on days 1, 7, 14, 21 and 28 after osteogenic induction, and stored at -20^{o}C. Cells were lysed in RIPA buffer and the ALP activity determined. Briefly, samples (50 µl) were incubated with 150 µl of assay solution including alkaline buffer, pNPP buffer and substrate pNPP at 37 ºC for 20 min. Calf intestinal phosphatase was used as positive control. Sodium hydroxide (200 µl, 0.1 M) was added to stop the reaction and the absorption at 405 nm was measured (triplicates of 100 µl from each tube) using a Victor^{3} 1420 multilabel counter (PerkinElmer Life Sciences, Wellesley, MA, USA).

Histology

Alizarin Red Staining - ~~Mineralization of the extracellular matrix was determined by Alizarin Red staining. Cells were plated in triplicate in osteogenic medium with medium change every 3 days. At end-point, cells were washed with PBS twice and fixed with 100% ethanol at room temperature for 20 min followed by several washes with diH_2O. Cultures were then stained with 0.1% alizarin red S (pH 5.5, adjusted by ammonium hydroxide) at room temperature for 30 min followed by several washes with diH_2O. Thereafter, cultures were air dried and documented on an Epson Perfection 1670 photo scanner (Seiko Epson, Nagano, Japan).~~

Alizarin Red Staining - Mineralization of the extracellular matrix was determined by Alizarin Red staining. Cells were plated in triplicate in osteogenic medium with medium change every 3 days. At end-point, cells were washed with PBS twice and fixed with 10% formalin for 10 min at room temperature followed by several washes with diH_2O. Cultures were then stained with Alizarin red at room temperature for 30 min followed by several washes with diH_2O. Thereafter, cultures were air dried and documented on an Epson Perfection 1670 photo scanner (Seiko Epson, Nagano, Japan).

Scanning electron microscopy

Cell and scaffold morphologies were studied under the scanning electron microscope (SEM). Scaffold surfaces were gold-sputtered and observed using 15kV accelerating voltage (Phillips XL30 FEG).

Statistical analyses

All the experiments were conducted in triplicate for three separate repeats. Significant differences ($P < 0.05$) were established using Student's *t* test.

RESULTS

Differentiation into the adipogenic and osteogenic lineage (2D culture)

Osteogenic induction

Osteogenic differentiation was monitored by light microscopy, histomorphology, immunohistology, and scanning electron microscopy (SEM). Following induction, H&E staining revealed the change in morphology of MPCs undergoing osteogenesis in 2D cultures (Fig. 2A-C), compared with the control groups (Fig. 2D-F) which maintained a more elongated morphology and appeared to have proliferated to a higher extent than their induced counterparts. ~~and a~~Alizarin red staining revealed increasing amounts of orange-red stained calcium deposits over the culture period (Fig. 2G-I) with no evidence of calcium deposition over the time course for the non-induced cells 9Fig. J-L)~~.~~ ~~Such osteogenic differentiation was also evident by scanning electron microscopy by day 28 after induction (data not shown).~~ Osteogenesis was further confirmed by the expression of type I collagen, demonstrated by immunohistochemistry on samples collected after 28 days (Fig. 3B). Both the cellular metabolism and proliferation (Fig. 4) of the osteo-induced cultures reached a peak between days 17 and 19, before declining. This was in contrast to the metabolic and proliferation profile of the non-induced samples, which showed an upward trend throughout the assay period (Fig. 4).

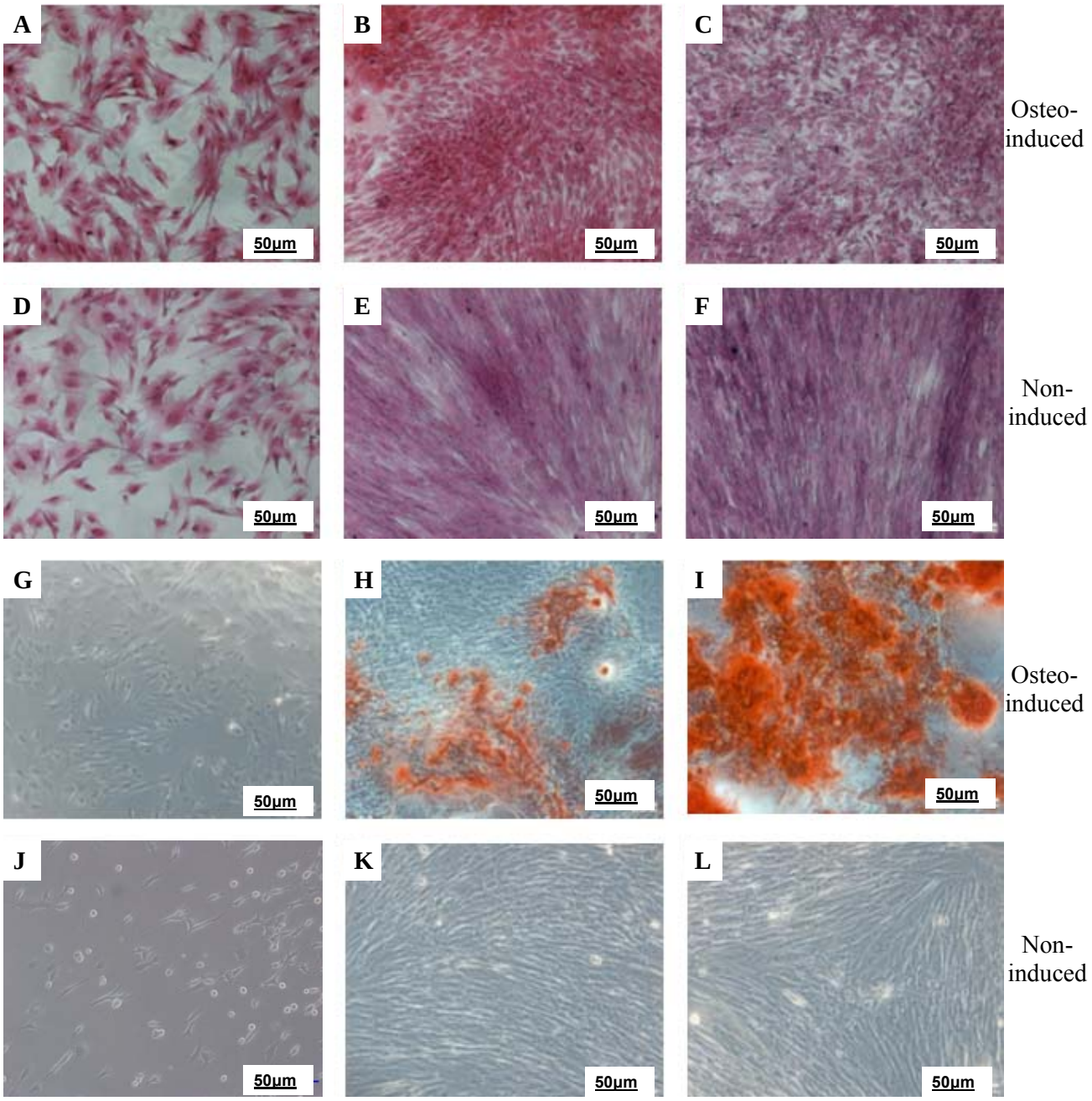

Figure 2. H&E (A-F) and Alizarin red (G-L) staining of osteo-induced (A-C, G-I) and non-induced cells (D-F, J-L) on days 1, 14 and 28 respectively (100X).

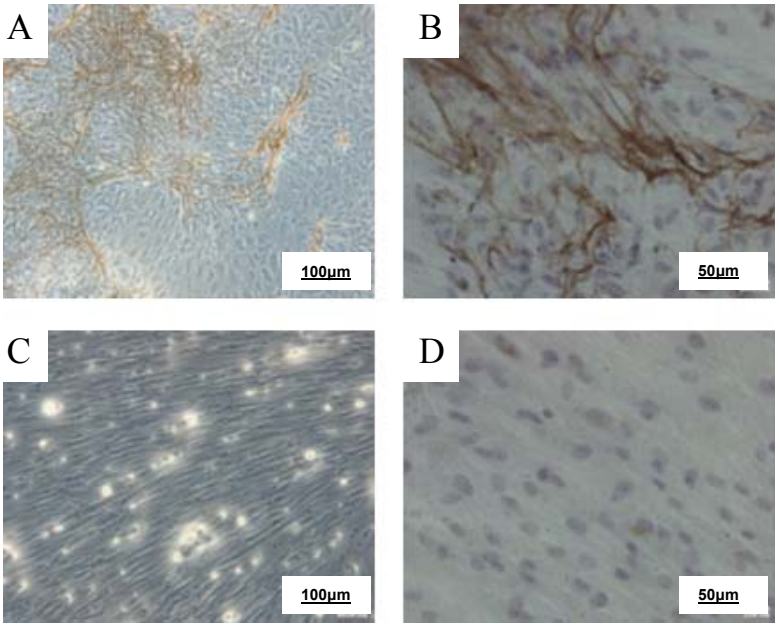

Figure 3. Type I collagen immunostaining performed on osteo-induced (A&B) and non-induced cells (C&D) on day 28.

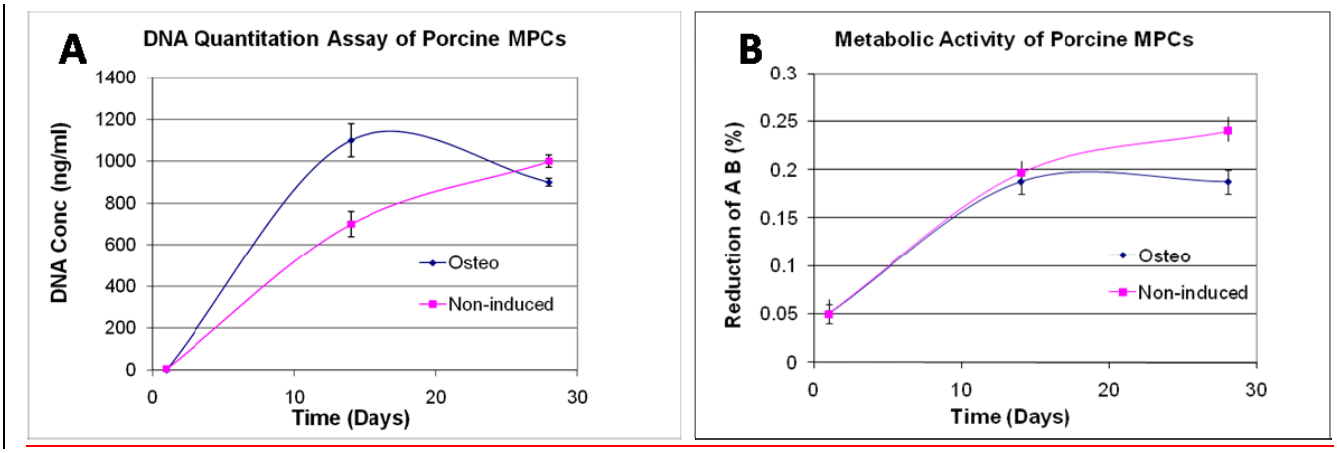

Figure 4. Graphs showing dsDNA quantitation (A) and metabolic activity (B) of porcine MPC undergoing osteogenic induction over a period of 28 days.

Adipogenic induction

Following adipogenic induction, H&E staining revealed changes from a fibroblastic, to a flat and oval cell morphology (data not shown). Cells at day 42 of induction revealed characteristic lipid droplets that filled the cytoplasm of the cells (Fig. 5A-B). Oil-Red-O staining was also performed to confirm their presence, and results show that lipid droplets started appearing 28 days after the cultures were

induced (Fig. 5C). By day 42 of induction, a greater proportion of the ~~BMSC~~MPCs contained lipid droplets, and there were also a greater number of lipid droplets within each cell (Fig 5D). Thus porcine ~~BMSC~~MPCs were able to differentiate along the adipogenic lineage when cultured with adipogenic induction media.

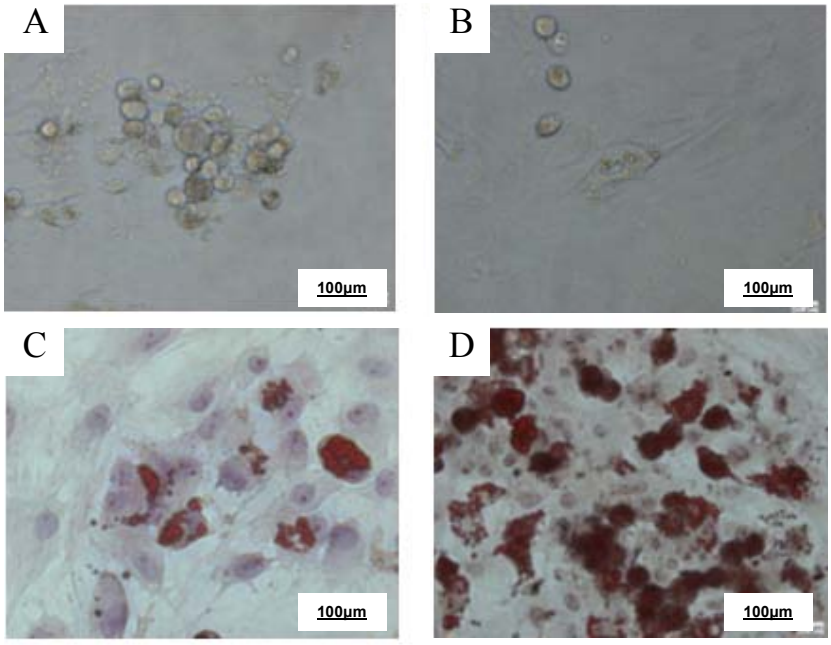

Figure 5. Photomicrographs showing adipo-induced cells on day 42. Lipid vacuoles within the cells **(A, B)**. Oil Red O staining of adipo-induced cells on days 28 (C) and 42 (D).

Figure 6B~~A~~ depicts the metabolic activity of adipo-induced and control cultures, an induction which rose to a peak between days 25 - 28 before declining, whereas the cell numbers of the adipo-induced cells were markedly lower than that of the non-induced cells over the culture period (Fig 6A~~B~~). By day 42, cell numbers in the non-induced samples had reached a plateau whereas those in the adipo-induced samples were still increasing. This is in contrast to the osteo-induced samples (Fig. 4) where cell numbers in induced and non-induced cultures did not differ significantly over the assay period.

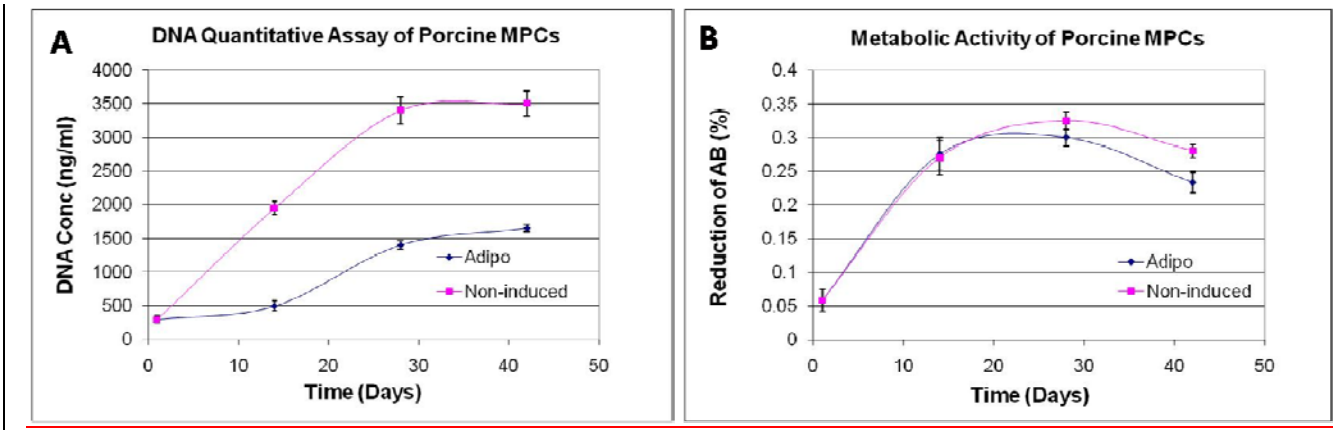

Figure 6. Graphs showing dsDNA quantitation (A) and metabolic activity (B) of porcine MPC undergoing adipo-induction over a period of 42 days.

Collagen Lyophilisation of PCL-TCP scaffolds and Heparin Adsorption:

In order to improve cell-seeding efficiency, and to act as a carrier for our biomolecule: heparin, PCL-TCP scaffolds were functionalised with lyophilised collagen type I. To determine the extent of collagen coating, scaffolds were viewed using scanning electron microscopy as depicted in Figure 7A&B. Alexaflour488 dye-labeled heparin that had been adsorbed to PCL-TCP scaffold before and after NaOH treatment is shown in Figure 7C&D, and viewed with fluorescence microscopy. NaOH-treated scaffolds which were then lyophilized with collagen yielded excellent surface modification of the PCL-TCP scaffolds following alkali treatment, and a highly favorable architectural organization of the collagen which was conducive to cell attachment and proliferation, as evidenced by the extensive and organized fluorescence along the collagen-coated scaffold struts (Fig. 7E).

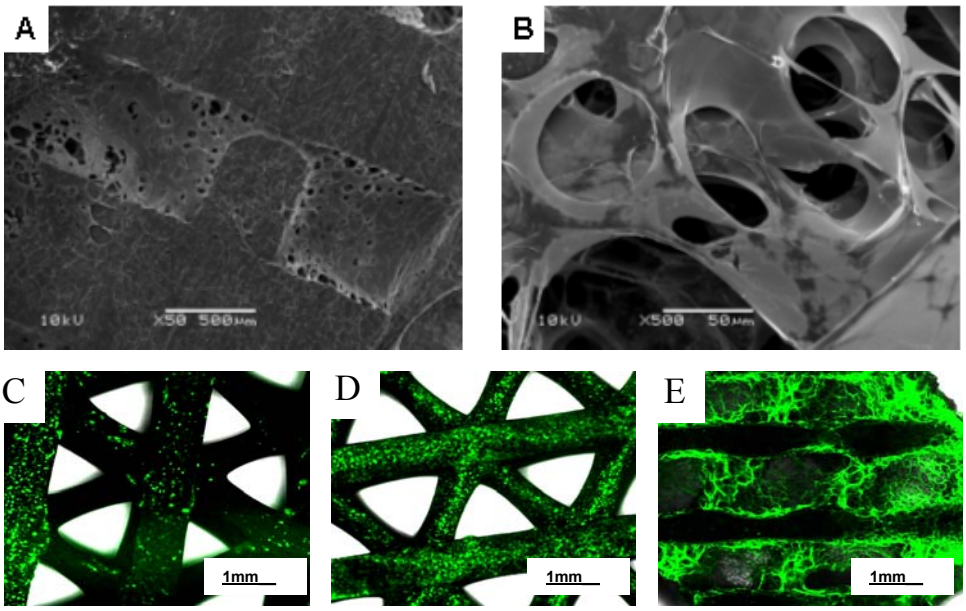

Figure. 7 Scanning electron microscopy images of lyophilised collagen (without cells) on the scaffolds (50X) (A) and 500X (B). Alexaflour488 dye labeled heparin which was adsorbed to PCL-TCP scaffold before (C) and after (D) NaOH treatment. NaOH-treated scaffolds after lyophilisation with collagen (E).

Osteogenic induction in heparin-adsorbed PCL-TCP-Col scaffolds (3D culture):

To ensure that the Porcine MPCs were adhered to the PCL-TCP-Col scaffolds either with or without exogenous heparin, samples were observed under light microscopy. The opaqueness of the scaffolds impeded the visibility of the struts, and thus the cells were visible mainly within the pores of the scaffolds. Fourteen to 28 days after induction, the cells that attached to the scaffolds started to proliferate and spread out on the surface of the struts, forming an interconnecting network of cells, remaining spindle-shaped. Migration of the cells towards the sides of the scaffold pores resulted in bridge formation, with cells on the opposite struts of the pores forming cell sheets. The cells within the cell sheets started to produce their own ECM components, appearing as cloudy areas under the light microscope (data not shown).

Similar to the situation observed under 2D culture conditions (Fig. 6A), the metabolic activity of the porcine ~~BMSC~~MPCs on both the PCL-TCP-Col and PCL-TCP-Col-heparin scaffolds increased from day 1 to day 14, before decreasing slightly on day 28 (Fig. 8A). Similar metabolic activity was

observed for both scaffold groups on days 1 and 14 after induction. By day 28 however, the metabolic activity of the cells on the PCL-TCP-Col scaffolds remained relatively unchanged from day 14, while that of the PCL-TCP-Col-heparin scaffolds showed a marked decrease. DNA quantitation revealed a significant increase from days 1 to 14, indicating cell proliferation (Fig 8B). Alkaline phosphatase activity of both the PCL-TCP-Col and PCL-TCP-Col-heparin groups remained fairly constant from day 1 – day 7 after induction, before rising to reach a peak at day 14 (Fig 8C). A decreasing trend was then observed between day 14 and day 28. No significant difference was observed between the two groups at all time points except that of day 21, where the ALP expression of the PCL-TCP-Col-heparin group was significantly lower than that of the PCL-TCP-Col group ($p<0.05$).

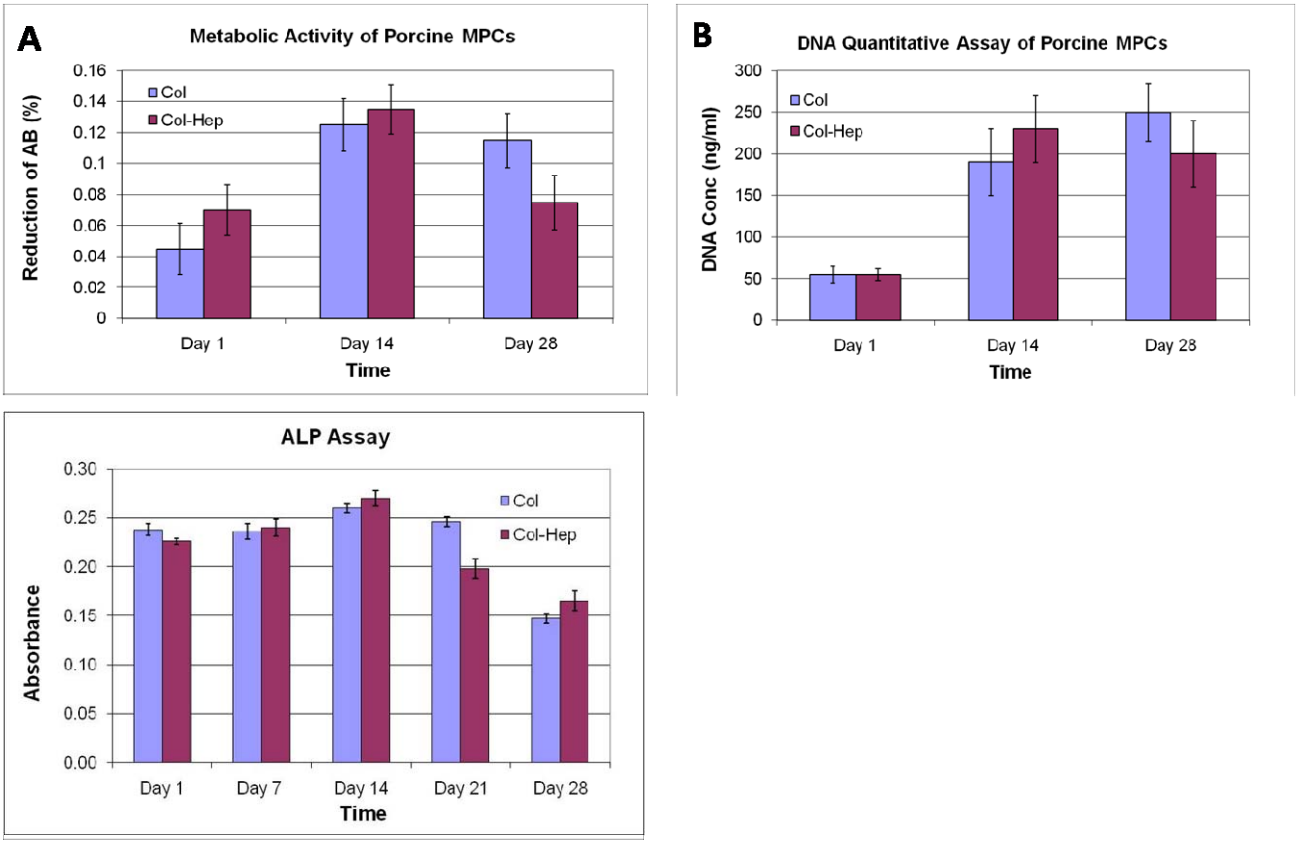

Figure 8. Metabolic activity of porcine MPCs following osteo-induction (A) dsDNA quantitation (B) and alkaline phosphatase expression (C) in collagen and collagen-heparin coated scaffolds, over a period of 28 days.

Reconstructed images of the 3D cell-scaffold constructs taken using confocal laser microscopy are depicted in Figure 9E-H. Viable cells are seen stained green by fluorescein diacetate (FDA), with cell attachment and spreading over the scaffold surface. The cells were observed in different planes, illustrating that there were cells on the surface of the struts as well as deeper within the scaffold pores. Good viability was observed, as shown by the larger proportion of green than red staining in both groups. Using SEM, the cells were seen to have colonized and formed layers over the scaffold surface, consequently leading to an inability to observe the initial meshwork of collagen on the surface of the scaffolds (Fig. 9A-D). Features such as cell sheets and cell bridges between the struts of the scaffold could be observed in both the PCL-TCP-Col and PCL-TCP-Col-heparin groups by day 14, later followed by cell bridging and formation of dense layers of cell sheets, supporting the idea that porcine ~~BMSC~~MPCs show good affinity for both groups of PCL-TCP scaffolds. Alizarin red staining (Figure 9I-L) demonstrated orange-red stains of calcium deposits within the small section of tissues after 28 days of osteogenic induction.

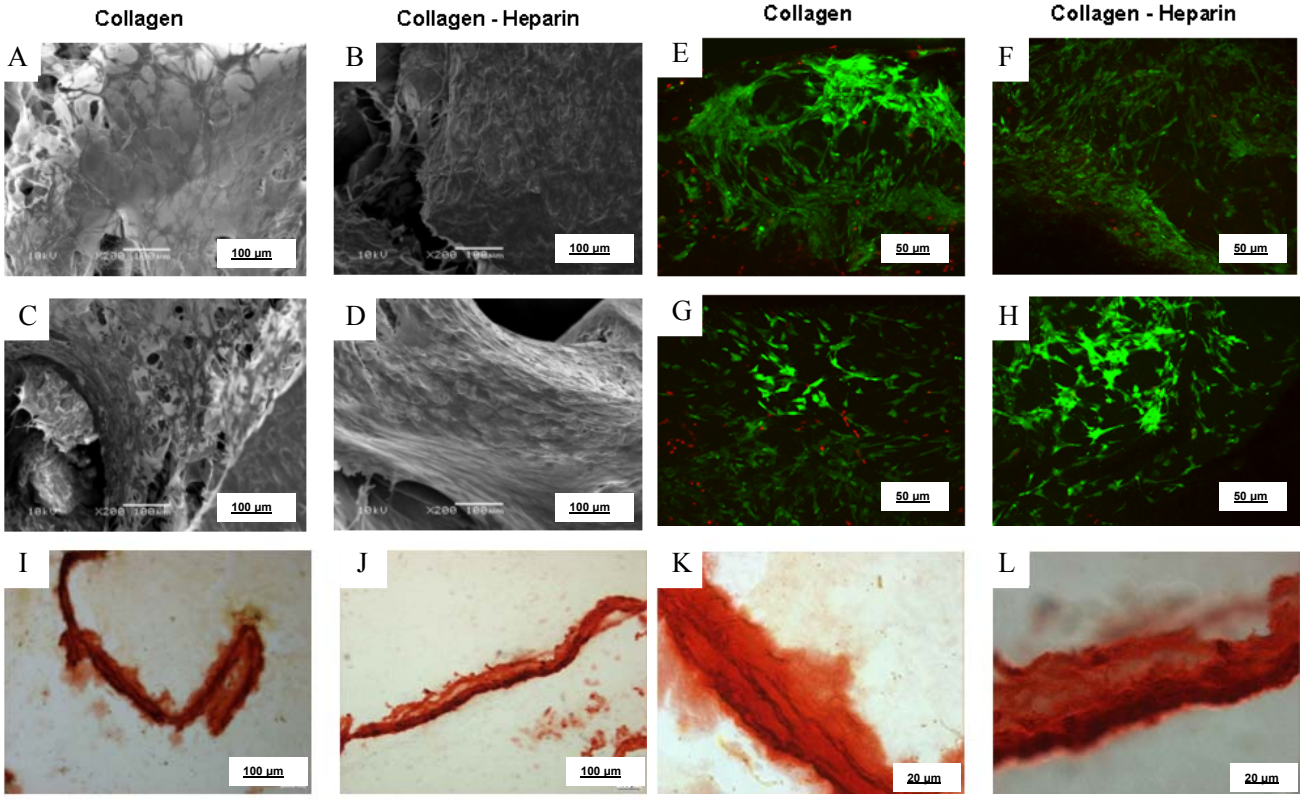

Figure 9. Scanning electron microscopy images of porcine ~~BMSC~~MPC in collagen (A&C) and collagen-heparin (B&D) coated scaffolds. Confocal Laser Microscopy photos of porcine ~~BMSC~~MPC in collagen (E&G) and collagen-heparin (F&H) coated scaffolds. Alizarin red staining of osteogenically induced porcine ~~BMSC~~MPC in collagen (I&K) and collagen-heparin (J&L) coated scaffolds. All images at day 28.

DISCUSSION

Although the induced differentiation of human marrow-derived stromal cells, as well as other species, has been well documented, little research has been done on the characterisation and differentiation of porcine bone marrow cells. Confirming the report of Ringe *et al* [14], porcine MPCs treated here with dexamethasone, a synthetic glucocorticoid, demonstrated the ability to undergo lineage-specific differentiation. We sought to more fully determine the capacity of porcine MPCs to differentiate down the osteogenic lineage within well characterised 3D PCL-TCP-Col scaffolds The mesenchymal progenitor cells attached avidly to the surfaces of 3D PCL-TCP-Col scaffolds as revealed by light and scanning electron microscopy, and were able to proliferate to fill the spaces on, as well as within, the pores of the construct. We utilised collagen type I lyophilised matrix to provide an interconnected meshwork leading to a larger surface area, which acted to increase seeding efficiency. The collagen also functioned as a carrier matrix for the incorporation of heparin. Our aim to investigate whether heparin would act as a possible promoter of osteogenesis was not fulfilled at the doses chosen for this study. Despite the heparin exerting no significant effect however, we did successfully utilise this well characterised scaffold system and the potential exists for the incorporation and release of other biomolecules from this system.

Our study demonstrated cell metabolism and proliferation to increase on the scaffolds between days 1 and 14. The 3D culture conditions also resulted in the active synthesis and deposition of ECM, indicating that a cell-cell and cell-ECM interconnective network was formed. The effect of heparin on the proliferation in the 3D environment showed a similar trend for both the metabolic activity as well as the DNA concentration of the cells in both the PCL-TCP-Col and PCL-TCP-Col-heparin groups over 28 days. There was positive alizarin red staining for calcium deposition observed in both groups, similar to that observed in the osteogenically-induced group in the 2D study. Although it was expected that the TCP scaffolds would yield a positive alizarin red stain by virtue of their composition, close

observation revealed that the sheets attached to the scaffolds also stained positive, supporting the proposition that calcification had occurred in the cells.

No noticeable difference however could be detected in the extent of osteogenesis of the two scaffold groups (heparin coated and non-coated) in this study. Both groups stained positive with alizarin red, and ALP activity over a period of 28 days also showed similar trends, rising to reach a peak after day 14 of induction, before declining. ALP is a non-specific, but well characterized early marker, and its increase is associated with osteoblastic differentiation. A recent study by Hausser et al. [11] reported that heparin has a biphasic effect on osteoblast-like cells – high concentrations of heparin (≥ 5 µg/ml) caused a reduction in cell numbers and inhibited matrix deposition and mineralization, while low concentrations (5 - 500 ng/ml) promoted proliferation, matrix deposition and mineralization. In contrast, heparin coated onto PCL-TCP-Col scaffolds did not show any significant effects on the proliferation and osteogenic activity of porcine ~~BMSC~~MPCs. It may be that the level of induction by the osteogenic media pushed the cells towards osteogenic differentiation to an extent that made it impossible to detect any influence brought about by the adsorbed heparin. The osteoconductive TCP present in both groups of scaffolds, as well as lyophilized collagen on the scaffolds might have compounded this effect; a study by Mizuno et al. [19] found that type I collagen matrix gels could induce osteoblastic differentiation of bone marrow cells. With so many factors affecting osteogenic lineage progression, any additional effects of heparin on differentiation may not be detectable by the relatively insensitive histological staining and ALP assays

The lack of effect of heparin throughout this study is not altogether surprising however. Depending on the context of presentation, heparin is a often a poor mimic of tissue-specific heparin sulfate (HS); this is seen clinically where its hypersulfated chains are just specific enough to interfere with a host of HS-dependent metabolic functions, but seldom specific enough to drive appropriate growth factor or cell-cell interactions [5, 6, 11]. *In vitro* studies have suggested that a vast repertoire of growth factors require

HSPGs as co-receptors to bind to their signaling receptors [20, 21]. The fibroblast growth factors (FGFs), of which there are over 20 forms, are thought of as the quintessential HS-dependent growth factors, and in the human osteogenic syndromes of craniosynostosis and dwarfism, FGF receptor mutants show the results of defects in FGF receptor signaling [22-26]. The FGF mitogenic family binds to HS chains with moderate affinity [27]. The interaction in turn catalyses the binding of the FGFs to their cognate, cell surface tyrosine kinase receptors, allowing signal transduction to take place. Early studies in this area mistakenly concluded that HSPGs play no direct role in FGF-receptor interactions but rather, like heparin in tissue culture, act to protect FGFs from denaturation by sequestering them in the ECM [28, 29]. Simultaneous discoveries that employed techniques that interfered with cell glycosaminoglycan (GAG) expression [30, 31] revealed that, in fact, FGF bioactivity was HS-dependent. A similar schema as been shown for HS, and the other major bone stem cell-active factors, the family of BMPs, and their threonine-serine kinase BMP receptors [32]. HS thus acts to concentrate these osteogenically-active growth factors close to cells, protect them from extracellular proteases, shepherd them to the cell surface, and facilitate binding to their specific receptors. Currently, it is posited that a vast array of other polypeptides, including heparin-binding epidermal growth factor (EGF)-like growth factor, hepatocyte growth factor, and the Wnts [33-35], to name just a few, are similarly dependent on particular HS species for their activities. The exact roles of HS for the recognition/coupling of ECM-resident adhesive glycoproteins such as laminin, fibronectin, or thrombospondin, or for HS-dependent CAM/cadherin cell-cell binding remains unclear.

However, one thing that has become clear is that relatively specific HS forms exist that bring specific ligands into register with their specific receptor isoforms [20, 36]. Thus future experiments might concentrate on delivering not heparin, but tissue-relevant forms of HS that are known to control stem/progenitor cells by virtue of their effects on developmental signaling cascades. We have already shown that HS can be successfully microencapsulated and still retain its bioactivity [37]. The challenge of successfully delivering them into active wound sites thus remains a major therapeutic goal. In the

context of bone tissue engineering, the delivery vehicle would need to comprise a scaffold, meeting the various, aforementioned criteria including appropriate porosity, strength, osteoinductivity, and biocompatability. In the present case of our PCL-TCP-Col scaffolds, these show great potential for fulfilling these criteria, especially when used in combination with different biomolecules and cell types, and this may be vital in the future to the successful regeneration of critical bone defects that would otherwise remain non-restored.

ACKNOWLEDGEMENTS

This research was carried out with support from the ASTAR grant BMRC 04/1/21/19/308 (R-397-000-613-305)

REFERENCES

1. Blair, H.; Sun, L.; Kohanski, R. A., Balanced Regulation of Proliferation, Growth, Differentiation, and Degradation In Skeletal Cells. *Ann N Y Acad Sci* **2007**, 1116, (1), 165–173.
2. Cool, S. M.; Nurcombe, V., The osteoblast-heparan sulfate axis: control of the bone cell lineage. *Int J Biochem Cell Biol* **2005,** 37, (9), 1739-45.
3. Cool, S. M.; Nurcombe, V., Heparan sulfate regulation of progenitor cell fate. *J Cell Biochem* **2006,** 99, (4), 1040-51.
4. Kilcoyne, M.; Joshi, L., Carbohydrates in therapeutics. *Cardiovasc Hematol Agents Med Chem* **2007,** 5, (3), 186-97.
5. Kock, H. J.; Handschin, A. E., Osteoblast growth inhibition by unfractionated heparin and by low molecular weight heparins: an in-vitro investigation. *Clin Appl Thromb Hemost* **2002,** 8, (3), 251-5.
6. Zhang, F.; McLellan, J. S.; Ayala, A. M.; Leahy, D. J.; Linhardt, R. J., Kinetic and structural studies on interactions between heparin or heparan sulfate and proteins of the hedgehog signaling pathway. *Biochemistry* **2007,** 46, (13), 3933-41.
7. Mazanec, D. J.; Grisanti, J. M., Drug-induced osteoporosis. *Cleve Clin J Med* **1989,** 56, (3), 297-303.
8. Squires, J. W.; Pinch, L. W., Heparin-induced spinal fractures. *Jama* **1979,** 241, (22), 2417-8.
9. Wawrzynska, L.; Tomkowski, W. Z.; Przedlacki, J.; Hajduk, B.; Torbicki, A., Changes in bone density during long-term administration of low-molecular-weight heparins or acenocoumarol for secondary prophylaxis of venous thromboembolism. *Pathophysiol Haemost Thromb* **2003,** 33, (2), 64-7.
10. Rajgopal, R.; Butcher, M.; Weitz, J. I.; Shaughnessy, S. G., Heparin synergistically enhances interleukin-11 signaling through up-regulation of the MAPK pathway. *J Biol Chem* **2006,** 281, (30), 20780-7.
11. Hausser, H. J.; Brenner, R. E., Low doses and high doses of heparin have different effects on osteoblast-like Saos-2 cells in vitro. *J Cell Biochem* **2004,** 91, (5), 1062-73.
12. Caplan, A. I., Adult mesenchymal stem cells for tissue engineering versus regenerative medicine. *J Cell Physiol* **2007**.

13. Zou, X.; Li, H.; Baatrup, A.; Lind, M.; Bunger, C., Engineering of bone tissue with porcine bone marrow stem cells in three-dimensional trabecular metal: in vitro and in vivo studies. *APMIS Suppl* **2003**, (109), 127-32.
14. Ringe, J.; Kaps, C.; Schmitt, B.; Buscher, K.; Bartel, J.; Smolian, H.; Schultz, O.; Burmester, G. R.; Haupl, T.; Sittinger, M., Porcine mesenchymal stem cells. Induction of distinct mesenchymal cell lineages. *Cell Tissue Res* **2002,** 307, (3), 321-7.
15. Hsu, S. H.; Yen, H. J.; Tseng, C. S.; Cheng, C. S.; Tsai, C. L., Evaluation of the growth of chondrocytes and osteoblasts seeded into precision scaffolds fabricated by fused deposition manufacturing. *J Biomed Mater Res B Appl Biomater* **2007,** 80, (2), 519-27.
16. Hutmacher, D. W.; Woodruff, M. A., Fabrication and Characterisation of Scaffolds via Solid Free Form Fabrication Techniques. In *Handbook of Fabrication and Processing of Biomaterials* CRC Press/Taylor and Francis Group: 2007; Vol. 1.
17. Zhou, Y.; Chen, F.; Ho, S. T.; Woodruff, M. A.; Lim, T. M.; Hutmacher, D. W., Combined marrow stromal cell-sheet techniques and high-strength biodegradable composite scaffolds for engineered functional bone grafts. *Biomaterials* **2007,** 28, (5), 814-24.
18. Osmond, R. I.; Kett, W. C.; Skett, S. E.; Coombe, D. R., Protein-heparin interactions measured by BIAcore 2000 are affected by the method of heparin immobilization. *Anal Biochem* **2002,** 310, (2), 199-207.
19. Mizuno, M.; Fujisawa, R.; Kuboki, Y., Type I collagen-induced osteoblastic differentiation of bone-marrow cells mediated by collagen-alpha2beta1 integrin interaction. *J Cell Physiol* **2000,** 184, (2), 207-13.
20. Guimond, S. E.; Turnbull, J. E., Fibroblast growth factor receptor signalling is dictated by specific heparan sulphate saccharides. *Curr Biol* **1999,** 9, (22), 1343-6.
21. Turnbull, J.; Powell, A.; Guimond, S., Heparan sulfate: decoding a dynamic multifunctional cell regulator. *Trends Cell Biol* **2001,** 11, (2), 75-82.
22. Ibrahimi, O. A.; Eliseenkova, A. V.; Plotnikov, A. N.; Yu, K.; Ornitz, D. M.; Mohammadi, M., Structural basis for fibroblast growth factor receptor 2 activation in Apert syndrome. *Proc Natl Acad Sci U S A* **2001,** 98, (13), 7182-7.
23. Itoh, N.; Ornitz, D. M., Evolution of the Fgf and Fgfr gene families. *Trends Genet* **2004,** 20, (11), 563-9.
24. Naski, M. C.; Ornitz, D. M., FGF signaling in skeletal development. *Front Biosci* **1998,** 3, d781-94.
25. Ornitz, D. M., FGF signaling in the developing endochondral skeleton. *Cytokine Growth Factor Rev* **2005,** 16, (2), 205-13.
26. Perlyn, C. A.; Morriss-Kay, G.; Darvann, T.; Tenenbaum, M.; Ornitz, D. M., A model for the pharmacological treatment of crouzon syndrome. *Neurosurgery* **2006,** 59, (1), 210-5; discussion 210-5.
27. Ornitz, D. M., FGFs, heparan sulfate and FGFRs: complex interactions essential for development. *Bioessays* **2000,** 22, (2), 108-12.
28. Gospodarowicz, D.; Cheng, J., Heparin protects basic and acidic FGF from inactivation. *J Cell Physiol* **1986,** 128, (3), 475-84.
29. Moscatelli, D., Basic fibroblast growth factor (bFGF) dissociates rapidly from heparan sulfates but slowly from receptors. Implications for mechanisms of bFGF release from pericellular matrix. *J Biol Chem* **1992,** 267, (36), 25803-9.
30. Rapraeger, A. C.; Krufka, A.; Olwin, B. B., Requirement of heparan sulfate for bFGF-mediated fibroblast growth and myoblast differentiation. *Science* **1991,** 252, (5013), 1705-8.
31. Yayon, A.; Klagsbrun, M.; Esko, J. D.; Leder, P.; Ornitz, D. M., Cell surface, heparin-like molecules are required for binding of basic fibroblast growth factor to its high affinity receptor. *Cell* **1991,** 64, (4), 841-8.
32. Irie, A.; Habuchi, H.; Kimata, K.; Sanai, Y., Heparan sulfate is required for bone morphogenetic protein-7 signaling. *Biochem Biophys Res Commun* **2003,** 308, (4), 858-65.

33. Aviezer, D.; Yayon, A., Heparin-dependent binding and autophosphorylation of epidermal growth factor (EGF) receptor by heparin-binding EGF-like growth factor but not by EGF. *Proc Natl Acad Sci U S A* **1994,** 91, (25), 12173-7.
34. Reichsman, F.; Smith, L.; Cumberledge, S., Glycosaminoglycans can modulate extracellular localization of the wingless protein and promote signal transduction. *J Cell Biol* **1996,** 135, (3), 819-27.
35. Zioncheck, T. F.; Richardson, L.; Liu, J.; Chang, L.; King, K. L.; Bennett, G. L.; Fugedi, P.; Chamow, S. M.; Schwall, R. H.; Stack, R. J., Sulfated oligosaccharides promote hepatocyte growth factor association and govern its mitogenic activity. *J Biol Chem* **1995,** 270, (28), 16871-8.
36. Guimond, S.; Turner, K.; Kita, M.; Ford-Perriss, M.; Turnbull, J., Dynamic biosynthesis of heparan sulphate sequences in developing mouse brain: a potential regulatory mechanism during development. *Biochem Soc Trans* **2001,** 29, (Pt 2), 177-81.
37. Luong-Van, E.; Grondahl, L.; Nurcombe, V.; Cool, S., In vitro biocompatibility and bioactivity of microencapsulated heparan sulfate. *Biomaterials* **2007,** 28, (12), 2127-36.